Cold Plasma Reticulation of Shape Memory Embolic Tissue Scaffolds

Landon D. Nash, Nicole C. Docherty, Mary Beth B. Monroe, Kendal P. Ezell, James K. Carrow, Sayyeda M. Hasan, Akhilesh K. Gaharwar, Duncan J. Maitland*

Polyurethane shape memory polymer (SMP) foams are proposed for use as thrombogenic scaffolds to improve the treatment of vascular defects, such as cerebral aneurysms. However, gas blown SMP foams inherently have membranes between pores, which can limit their performance as embolic tissue scaffolds. Reticulation, or the removal of membranes between adjacent foam pores, is advantageous for improving device performance by increasing blood permeability and cellular infiltration. This work characterizes the effects of cold gas plasma reticulation processes on bulk polyurethane SMP films and foams. Plasma-induced changes on material properties are characterized using scanning electron microscopy, uniaxial tensile testing, goniometry, and free strain recovery experiments. Device specific performance is characterized in terms of permeability, platelet attachment, and cell–material interactions. Overall, plasma reticulated SMP scaffolds show promise as embolic tissue scaffolds due to increased bulk permeability, retained thrombogenicity, and favorable cell–material interactions.

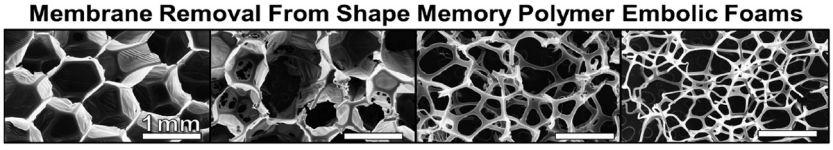

1. Introduction

Polyurethane shape memory polymer (SMP) foams have shown promise as effective embolic materials that address current embolization technique limitations by reducing the number of devices needed for treatment and improving long term healing outcomes.[1–4] These low density materials can be radially compressed and programmed into a low volume configuration to facilitate minimally invasive catheter delivery to a diseased vascular anatomy. Once delivered, the material can be stimulated with heat to expand to its primary configuration for effective volumetric filling and flow stasis, leading to embolization. These materials demonstrate excellent biocompatibility for aneurysm embolization applications, but additional material optimization is necessary to enable their use in other applications, such as peripheral embolization devices to treat chronic venous insufficiency.[4]

The implanted SMP foam is intended to serve as a tissue scaffold for thrombus formation and subsequent cell-mediated healing. However, gas blown foams inherently have membranes between pores, which can limit their performance as embolic tissue scaffolds.[5] Namely, implanted foams without interconnected pores can limit cellular infiltration during healing. Low permeability foams can also generate large pressure gradients in circulation, leading to potential device failure or migration after deployment in peripheral vasculature.

Reticulation, or the removal of membranes between adjacent foam pores, is advantageous for increasing foam permeability to improve material performance. Controlled reticulation of SMP foams would provide multiple benefits, such as an optimized surface area to volume ratio for intrinsic pathway-triggered blood coagulation and flow stagnation within the foam to produce

L. D. Nash, N. C. Docherty, Dr. M. B. B. Monroe, K. P. Ezell, J. K. Carrow, Dr. S. M. Hasan, Prof. A. K. Gaharwar, Prof. D. J. Maitland
Biomedical Engineering, Texas A&M University
5045 Emerging Technologies Building, 3120 TAMU
College Station, TX 77843, USA
E-mail: djmaitland@tamu.edu

DOI: 10.1002/marc.201600268

thrombogenic fluid shear rates.[6–8] Additionally, reticulated foams would allow for cellular infiltration as the body heals the thrombus within the foam.[9]

Traditional reticulation processes are too aggressive to use with ultralow density polyurethane SMP foams (≈0.015 g cc^{-1}). Attempts to reticulate the proposed polyurethane SMP foam using commercial techniques, such as acid etching, concussion, mechanical cycling, and combustion, resulted in significantly decreased mechanical integrity. For example, acid etching led to densification of the foam morphology, and concussion/combustion techniques led to complete material obliteration. A mechanical reticulation method that utilizes a floating array of weighted flexible pins to preferentially puncture foam membranes was previously reported as an effective reticulation method for ultralow density SMP foams with demonstrated utility in vessel occlusion.[10] Alternatively, cold gas plasma can be used for SMP foam reticulation. The proposed process uses a reactive oxygen (O_2) and tetrafloromethane (CF_4) plasma, commonly used to etch features for microelectronics, to nonthermally degrade and volatize high surface area membranes and reticulate SMP foam structures.[11–14]

Plasma processes have been widely used to alter the surface chemistry of biomaterials.[15–18] Many of these processes increase surface hydrophilicity for enhanced cell attachment.[19–21] Other studies are aimed to modify the interior surfaces of porous structures.[22–24] We hypothesize that the proposed plasma treatment can be utilized to reticulate foams in a controlled manner. Previously, a group used H_2O_2 plasma to sterilize SMP foams with an observed increase in pore interconnectivity.[25] Fu et al. also observed increases in porosity when treating polyurethane substrates with an active screen plasma.[26] However, no studies have explicitly focused on using plasma to tune the opening of porous structures. This work characterizes the effects of cold gas plasma reticulation processes on bulk polyurethane SMP films and foams to enhance their tunability and expand their potential use as embolic scaffolds.

2. Experimental Section

2.1. Sample Preparation

SMP foams were prepared according to the protocol described by Singhal et al. with an isocyanate composition of 100 mol% trimethylhexamethylene diisocyanate and a hydroxyl equivalent mole ratio of 33:67 triethanolamine to *N*,*N*,*N*′,*N*′-tetrakis(2-hydroxypropyl)ethylenediamine.[5] The cured foams were cut with a resistive wire cutter into 50 × 50 × 25 mm blocks and washed to remove residual surfactants and catalysts. The previously reported cleaning protocol involved two 15 min sonication intervals in reverse osmosis (RO) water, one interval in a 20 vol% Contrad 70 solution in RO water (Decon Laboratories, King of Prussia, PA), and four 15 min intervals in RO water.[4] Cleaned samples were frozen in aluminum trays and lyophilized for 3 d. Dried foams were stored in polypropylene bags under desiccation.

Type IV SMP foam dog bones with thicknesses between 3 and 4 mm were prepared from bulk foam using a resistive wire cutter and mechanical punch. Wooden blocks were adhered to each end using epoxy to mitigate sample deformation in the tensile tester grips.

Neat SMP films were prepared with the same monomer ratios as the foam. The monomers were massed into a Flacktek speed mixing cup (Flacktek SpeedMixers, Landrum, SC) in a moisture controlled glovebox. The reaction components were then mixed at 3400 rpm for 2 min to create a single phase solution. Once mixed, the solution was poured into a polypropylene casting tray and oven cured by heating to 120 °C at a rate of 30 °C h^{-1} and holding at 120 °C for 1 h. Films were then cooled to ambient temperature, milled on a single side to a uniform thickness of 0.2 cm, and CO_2 laser-cut into 2 cm squares. The top face of the film that was in contact with air during curing was preserved for surface analysis. Cured films were stored in polypropylene bags under desiccation.

2.2. Plasma Reticulation

Plasma treatment was conducted using an Aurora 0350 Plasma Surface Treatment System (Plasma Technology Systems). Polymer foam blocks were fixed on a 12.5 cm tall aluminum mesh fixture centered on the back third of the reaction chamber. Polymer films were fixed to a 4.5 cm tall glass cuvette during treatment. Foam dog bones were taped to bridge two 4.5 cm tall glass cuvettes during treatment. The chamber was evacuated to a base pressure of 10 mTorr, and then O_2 and CF_4 process gasses were introduced into the chamber at 200 and 800 sccm, respectively, to bring the chamber to a pressure of 385 mTorr. Block foam samples were plasma treated at 300 W for 8 or 15 min for partial or full reticulation, respectively. Foam dog bones were plasma treated at 300 W for 1, 2, and 3 min to achieve increasing degrees of reticulation, with 3 min achieving full reticulation. Unless otherwise stated, all film samples were plasma treated with a 15 min process. All plasma-treated samples were stored in polyethylene bags under desiccation.

2.3. Scanning Electron Microscopy

Using a resistive wire cutter, foam samples were cut into 1 mm slices parallel (axial) and orthogonal (transverse) to the foaming axis. Each slice was mounted to a stage with carbon black tape and sputter coated for 90 s at 20 mA using a Cressington Sputter Coater (Ted Pella, Inc. Redding, CA). Samples were then visualized using a Joel NeoScope JCM-5000 Scanning Electron Microscope (SEM) (Nikon Instruments, Inc., Melville, NY).

2.4. Permeability

The porous media properties of the plasma-reticulated and untreated foams were measured using a permeability system

as previously reported and calculated using the Forchheimer–Hazen–Dupuit–Darcy Equation (1)

$$-\frac{\partial P}{\partial x} = \frac{\mu}{K} v_{\circ} + \rho C v_{\circ}^{2} \quad (1)$$

where, $\frac{\partial P}{\partial x}$ was the pressure gradient across the sample in the direction of flow (Pa m^{-1}), μ was the dynamic viscosity of the working fluid (Pa s), K was the permeability of the sample (m^2), $v_{\circ}$ was the Darcy velocity (flow rate divided by the cross-sectional area of the sample) (m s^{-1}), ρ was the density of the fluid (kg m^{-3}), and C was the form factor of the sample (m^{-1}).[10] Permeability, K, and form factor, C, were geometric parameters of the foam.

Permeability test samples (untreated, partially reticulated, and fully reticulated foams) were cut into 16 × 20 mm (OD × length) cylinders using a resistive wire cutter and biopsy punch. Each sample was slightly compressed to fit into a 30 × 19 × 16 mm (length × OD × ID) poly(methyl methacrylate) (PMMA) tube. UV cure epoxy (Dymax See-Cure 1202-M-SC, Dymax Corporation, Torrington, CT) was applied to the exterior surface of each cylindrical sample using a plastic spatula. Each sample was then placed into the PMMA tube with one end of the cylindrical sample flushed with the tube opening. The epoxy was UV cured for 30 s (Omni-Cure S1000, Lumen Dynamics, Canada) to bond the foam to the tube, and samples were stored under desiccation until testing.

Prior to permeability testing, each sample was sonicated in water for 1 h to remove air bubbles. The pressure drop across each foam sample was measured for at least 30 s at flow rates ranging from 0 to 750 mL min^{-1} (0–0.065 m s^{-1} Darcy velocity) to determine the K and C values of the foam. Each sample was initially measured with two digital 206 800 Pa pressure gauges (model #DPGWB-06, Dwyer Instruments, Michigan City, IN) to determine the peak pressure at maximum flow rate and to select the highest resolution transducer for subsequent tests. Based on these results, untreated and partially reticulated samples were analyzed using two 206 800 Pa absolute membrane pressure transducers (model #PX42G7-030GV, Omega Engineering, Inc.). Fully reticulated samples were analyzed using 2482 Pa (model #PX409-10WDWUV, Omega Engineering, Inc.) and 17 240 Pa (model #PX409-2.5DWUV, Omega Engineering, Inc.) differential pressure transducers.

A second-order least squares fit was applied to the pressure gradient versus Darcy velocity data to calculate K and C for each sample using Equation (1) with water at room temperature as the working fluid.

2.5. Tensile Testing

Uniaxial tensile tests were conducted at room temperature using an Insight 30 Material Tester (MTS Systems Corporation, Eden Prairie, MN) with a constant strain rate of 50 mm min^{-1}. Ultimate tensile strength (kPa), strain at break (%), and elastic modulus (kPa) were calculated from the stress–strain curve of each sample. Statistical analysis was conducted using a one-way analysis of variance (ANOVA) with Bonferroni's multiple comparisons test to the untreated control values.

2.6. Volumetric Expansion

Three cylindrical samples measuring 6 × 5 mm (OD × length) were prepared for each reticulation condition using a biopsy punch and razor blade. The foam samples were threaded axially onto a 200 micron diameter nitinol wire (NDC, Fremont, CA) and loaded into a SC150 Stent Crimper (Machine Solutions, Flagstaff, AZ) preheated to 100 °C. The samples were equilibrated for 15 min before being radially compressed. The samples remained constrained until they were cooled back to room temperature. Crimped foam over wire samples were stored under desiccation for a minimum of 24 h before expansion testing. Samples were mounted within a custom aluminum fixture that held the samples in the same imaging plane as a 12 mm measuring reference. The fixture was submerged in a 37 °C water bath and imaged at 1 min intervals for 15 min. Five diameter measurements were made along the length of each sample at each time point using ImageJ analysis software (National Institute of Health, MD, USA).

2.7. Static Water Contact Angle

Static water contact angle measurements were made on untreated and plasma treated films (300 W for 15 min) using a CAM 200 Goniometer (KSV Instruments) and drop volumes of 5 µL. Contact angles were measured at day 0, 7, 14, 21, and 28 post reticulation to examine hydrophobic relaxation of the sample. Three contact angles were measured using a Young/Laplace fitting model on four separate films for a total of 12 measurements for each process and time point.

2.8. Platelet Attachment

Bovine blood was acquired from a slaughterhouse immediately following animal sacrifice. To prevent coagulation, the blood was citrated in a 1 L glass jar with a 9:1 volume ratio of blood to 3.2% sodium citrate solution in phosphate buffered saline (PBS, pH 7.4). All blood studies were completed within 8 h of animal sacrifice.

Plasma treated (1 and 28 d posttreatment) and untreated films were rinsed three times with PBS and placed in a petri dish with the plasma-treated surface face up. The samples were submerged in citrated whole bovine blood and incubated for 1 h at 37 °C. After removing blood from the petri dish, the samples were rinsed three times with PBS and fixed with 3.7% glutaraldehyde at 37 °C for 2 h. A total of 16 images were captured for each sample surface condition using a brightfield microscope (Nikon Eclipse TE2000-S) at 40× magnification. Platelets were manually counted within each field of view, and platelet attachment density was calculated using known objective scaling.

2.9. Cell Culture

Cell–material interactions were evaluated on plasma treated (0 and 28 d posttreatment) and untreated films. Films (n = 3 per treatment condition) were sterilized under UV light for 3 h prior to seeding green fluorescent protein (GFP)-expressing 3T3 fibroblasts (NIH3T3/GFP, Cell Biolabs Inc., USA) on their surfaces at 200 cells mm^{-2}. At set time points (3 h, 1, 3, and 7 d), cells were

imaged using fluorescent microscopy (excitation: 488 nm, Nikon FN1 Upright Microscope, NY, USA). Cell area was quantified using ImageJ software over three images for each film condition with five representative cells measured per image. Cell proliferation was quantified over three images for each film condition using particle analysis in ImageJ with manual verification. Statistical analysis was conducted for the cell spreading and cell density data sets using two-way ANOVA with Bonferroni's multiple comparisons test.

3. Results and Discussion

3.1. Influence of Foam Morphology on Fluid Permeability

The plasma-induced changes in foam morphology are clearly visualized via SEM imaging, Figure 1A. Untreated foams have interpore membranes that are still largely intact. The partially reticulated foams have moderate membrane degradation with pinholes in the majority of the membranes, providing a degree of pore interconnectivity while maintaining a large surface area of membranes for blood–material interactions. Only a small percentage of membranes remain in the fully reticulated foams, while the foam struts remain intact. Full reticulation provides an open porous matrix for improved fluid permeability and cellular infiltration.

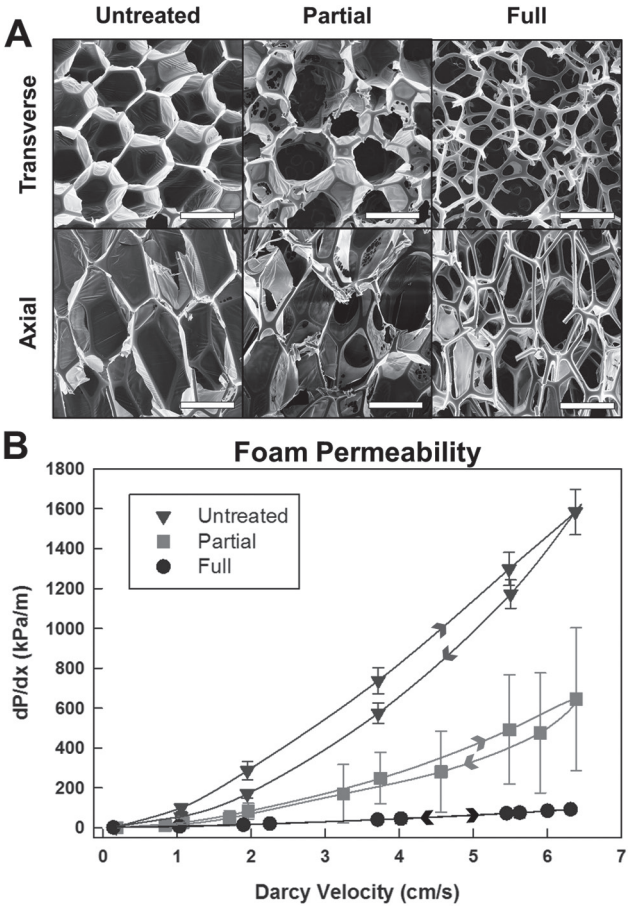

Figure 1. A) SEM images of untreated, partially reticulated (8 min treatment), and fully reticulated (15 min treatment) foams; scale bar is 1 mm. B) Pressure differential measurements across plasma reticulated and untreated foams with increasing and decreasing fluid flow rates; $n = 5$, mean ± standard deviation.

It is important to note the diffusive nature of the reticulation process. The larger foam block samples exhibited a slight reticulation gradient at higher reticulation levels, with the exterior of the foam being more reticulated than the center. All samples were taken from the center of SMP foam blocks where reticulation was most consistent between runs. However, the thinner dog bone samples did not exhibit this gradient effect, highlighting the need to tailor each process duration to the specific foam geometry. Additional considerations for process reproducibility include starting chamber temperature, RF shielding from multiple samples, sample fixturing, sample orientation, and spatial positioning within the reaction chamber.

Figure 1B quantifies the increases in material permeability due to plasma reticulation. For each reticulation condition, the permeability data are differentiated based on ramping the fluid velocity up or down to account for hysteresis. Untreated, partially reticulated, and fully reticulated foams had average form factor values of 2.91×10^5, 1.43×10^5, and 0.15×10^5 m^{-1}, respectively. Average permeability values for untreated, partially reticulated, and fully reticulated foams were 0.16×10^{-9}, 1.44×10^{-9}, and 2.55×10^{-9} m^2, respectively. Pressure drops across fully reticulated foams are over 16 times lower than those of untreated foams at Darcy velocities (5–7 cm s^{-1}) that correlate to those typically found in the saphenous vein (7 ± 2 cm s^{-1}).[27] Partially reticulated foam permeability fell between that of untreated and fully reticulated foams, consistent with the degree of observed membrane removal. The pressure gradient standard deviations for partially reticulated foams were significantly higher than those of untreated or fully reticulated foams due to the relative inhomogeneity of the reticulation.

3.2. Influence on Mechanical Integrity

Table 1 summarizes the tensile mechanical properties of plasma reticulated SMP foams. Increasing reticulation resulted in slight decreases in ultimate tensile stress with full reticulation causing the only statistically significant difference when compared to untreated foam ($p < 0.001$). Strain to failure slightly increased with reticulation, but "2 Partial" was the only reticulation condition determined to be statistically different from the untreated control

Table 1. Tensile mechanical properties of untreated and plasma reticulated foams ($n = 5$, average ± standard deviation, One-way ANOVA with Bonferroni's multiple comparisons test to untreated control; $^{*}p < 0.05$, $^{***}p < 0.001$).

Plasma duration [min]	Ultimate stress [kPa]	Strain at break [%]	Elastic modulus [kPa]
0 (Untreated)	106 ± 7	38 ± 6	490 ± 86
1 (Partial)	97 ± 14	42 ± 3	294 ± 62***
2 (Partial)	92 ± 6	46 ± 3*	241 ± 32***
3 (Full)	79 ± 3***	44 ± 4	202 ± 18***

($p < 0.05$). Ultimate stress and strain to failure are largely preserved because the foam struts that are left intact after reticulation contribute more to the tensile integrity and overall cross-sectional area of the foam when compared to membranes.

Significant decreases in elastic modulus were observed for each reticulation condition ($p < 0.001$). Membrane removal decouples the mechanical link between adjacent foam struts. This affords greater flexibility for each strut and results in an overall decrease in material stiffness. Comparable decreases in elastic modulus were also observed in mechanically reticulated SMP foams.[10]

3.3. In Vitro Shape Recovery

As seen in Figure 2, unreticulated foam samples had slow expansion rates at 37 °C with only 2 mm of expansion after 15 min of immersion. By comparison, partially reticulated foams expanded to almost 5 mm in diameter within 15 min. Fully reticulated samples achieved full shape recovery (6 mm diameter) in as little as 7 min.

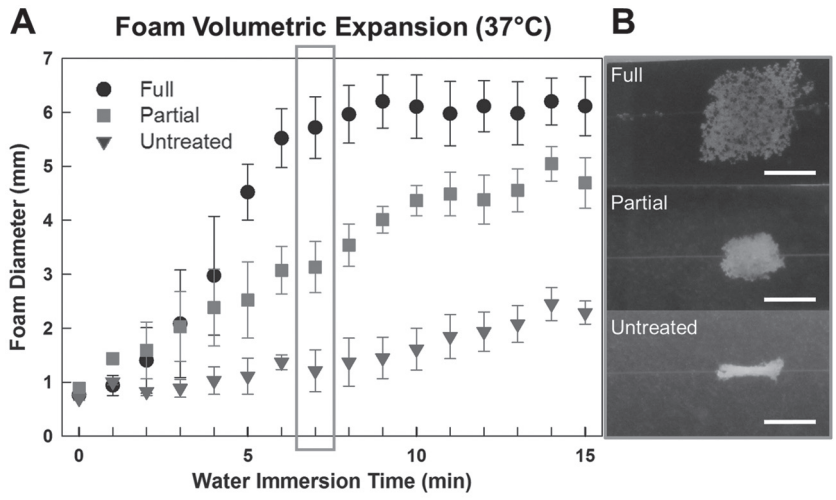

Figure 2. A) Unconstrained expansion measurements of plasma reticulated and untreated foam cylinders submerged in 37 °C water; $n = 15$, mean ± standard deviation. B) Still frame images of foams at 7 min of immersion. Scale bars are 5 mm.

These differences in expansion kinetics can be largely attributed to effects on moisture diffusion and moisture-plasticized glass transition temperature (T_g) depression. Actuation of SMP foams via plasticization is a known mechanism.[28,29] Increased permeability from membrane removal and increased surface hydrophilicity result in faster moisture diffusion throughout the material and a more rapid decrease in T_g, increasing the expansion rate at isothermal body conditions. These changes must be considered during device development to prevent premature foam expansion and excessive device friction within the delivery catheter.

3.4. Time-Dependent Surface Hydrophobicity and Thrombogenicity

Contact angle measurements were made on plasma treated films to confirm the hypothesis that increased surface hydrophilicity was a driver for increased expansion rates, Figure 3. On the day of plasma treatment, films were more hydrophilic with a contact angle of 45° ± 3° compared to untreated films with a contact angle of 96° ± 2°. However, the plasma treated surfaces exhibited hydrophobic recovery with an increased contact angle of 75° ± 4° after four weeks of storage in desiccated air.

Platelet attachment provides an indication of material thrombogenicity. As seen in Figure 3, platelet attachment correlated with increased surface hydrophobicity, with higher platelet attachment to four week aged films than to freshly plasma treated films. This result suggests that plasma treated devices intended for embolic applications should be aged prior to delivery to maximize their thrombogenicity.

3.5. Time-Dependent Cell Responses

Based on cell spreading morphology, cellular affinity to the plasma treated surface is demonstrated in as little as 3 h after seeding, Figure 4A. This initial adhesion enables significantly enhanced cell spreading on the plasma treated substrate at later time points, as seen after a week in vitro. As indicated by Figure 4B, the cells on the control film reach a threshold of cell area at ≈1 d of culture; however, cells on the plasma treated surface demonstrate highly extended pseudopodia

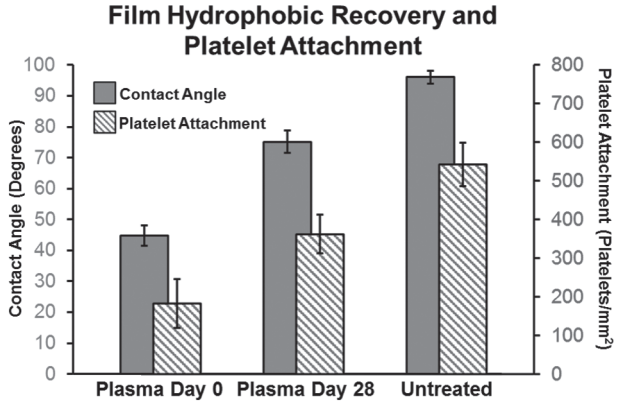

Figure 3. Water contact angles ($n = 12$, mean ± standard deviation) and platelet attachment quantification ($n = 16$ images, mean ± standard error) on SMP films 0 and 28 d post plasma treatment compared with untreated films.

with consistent increases in cell spreading over a week of culture. Similar fibroblast spreading behavior has been reported for tissue culture polystyrene with a comparable range of surface contact angles 63°–68°.[30] The observed decrease in cell spreading after four weeks post reticulation is attributed to the temporal hydrophobic recovery of the surface, Figure 3.

When compared to the untreated films, both plasma treated film conditions demonstrated higher average cell densities, especially at the later culture time points of 3 and 7 d, Figure 4C. However, only the third culture day "Plasma Day 28" sample showed a statistically significant difference ($p < 0.001$). Temporal changes in surface hydrophobicity did not have the same effect on cell proliferation as cell spreading. Future work should characterize other potential factors contributing to these cellular responses, including surface topography. The apparent surface affinity of the plasma treated film and interconnected porous morphology of the reticulated foam indicate the promise of these materials as embolic tissue scaffolds.

4. Conclusions

This work demonstrates control of bulk SMP embolic foam properties, including fluid permeability and volumetric expansion rate, using cold gas plasma reticulation. Observed surface effects are transient and demonstrate a tendency to recover toward baseline hydrophobicity over the course of several weeks. This surface relaxation has significant ramifications for device performance and should be considered in terms of specific device applications, packaging conditions, sterilization techniques, and shelf life. Overall, plasma treatment induced increases in pore interconnectivity and does not appear to impart deleterious

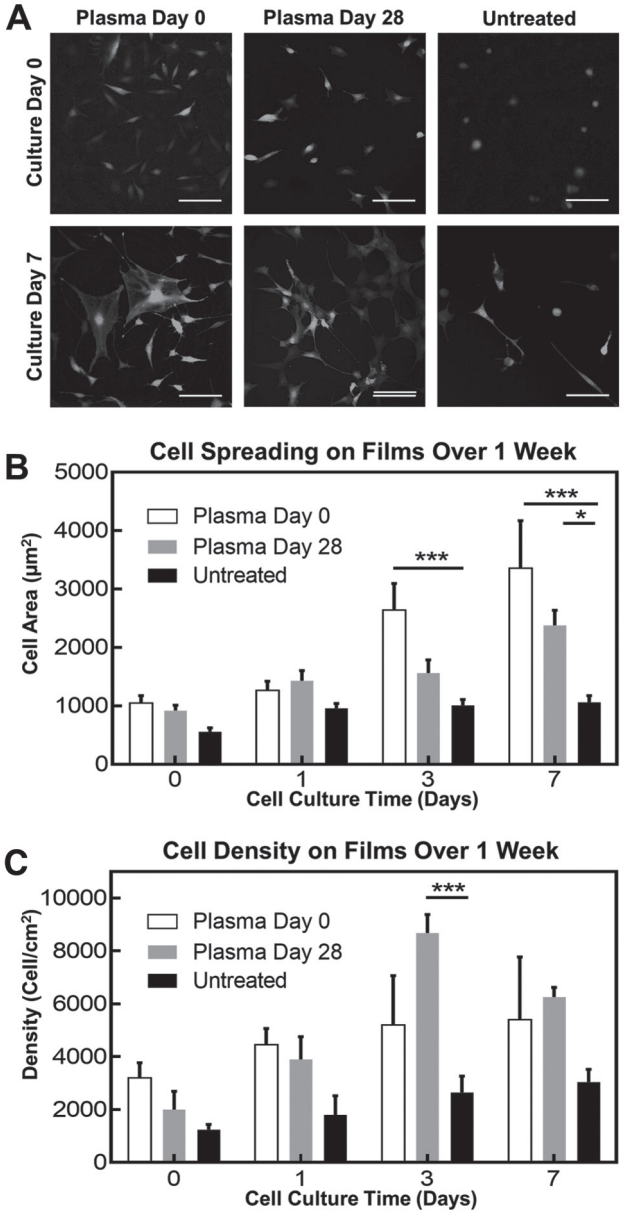

Figure 4. A) Fluorescent images of NIH3T3/GFP fibroblasts cultured on SMP films at 0 d and four weeks post plasma treatment compared to that on untreated SMP films after 3 h and one week of culture. Scale bar is 100 μm. B) Quantification of cell spreading over one week of culture on SMP films. $n = 5$ cells, three images per condition for a total of 15 measurements; mean ± standard error; Two-way ANOVA with Bonferroni's multiple comparisons test; $^{*}p < 0.05$ relative to untreated control; $^{***}p < 0.001$ relative to untreated control. C) Quantification of cell density over one week of culture on SMP films. Three images per condition; mean ± standard error; $^{***}p < 0.001$ relative to untreated control.

effects on cell–material interactions, indicating its utility for developing embolic tissue scaffolds. Furthermore, control over the pore interconnectivity and surface area to volume ratios of porous materials make this process useful for optimizing embolic medical device performance.

Supporting Information

Supporting Information is available from the Wiley Online Library or from the author.

Acknowledgements: This work was supported by the National Institutes of Health/National Institute of Biomedical Imaging and Bioengineering Grant R01EB000462, National Institutes of Health/National Institute of Neurological Disorders and Stroke Grant U01-NS089692, and National Science Foundation Graduate Research Fellowship Program Grant 1252521.

Received: May 8, 2016; Revised: July 26, 2016; Published online: August 29, 2016; DOI: 10.1002/marc.201600268

Keywords: foam reticulation; plasma surface modification; shape memory polymers

[1] W. Small, P. R. Buckley, T. S. Wilson, W. J. Benett, J. Hartman, D. Saloner, D. J. Maitland, *IEEE Trans. Biomed. Eng.* **2007**, *54*, 1157.
[2] D. J. Maitland, W. T. Small, J. M. Ortega, P. R. Buckley, J. Rodriguez, J. Hartman, T. S. Wilson, *J. Biomed. Opt.* **2007**, *12*, 030504.
[3] A. J. Boyle, T. L. Landsman, M. A. Wierzbicki, L. D. Nash, W. Hwang, M. W. Miller, E. Tuzun, S. M. Hasan, D. J. Maitland, *J. Biomed. Mater. Res., Part B: Appl. Biomater.* **2015**.
[4] J. N. Rodriguez, F. J. Clubb, T. S. Wilson, M. W. Miller, T. W. Fossum, J. Hartman, E. Tuzun, P. Singhal, D. J. Maitland, *J. Biomed. Mater. Res., Part A* **2014**, *102*, 1231.
[5] P. Singhal, J. N. Rodriguez, W. Small, S. Eagleston, J. Van de Water, D. J. Maitland, T. S. Wilson, *J. Polym. Sci., Part B: Polym. Phys.* **2012**, *50*, 724.
[6] J. M. Anderson, A. Rodriguez, D. T. Chang, *Semin. Immunol.* **2008**, *20*, 86.
[7] E. A. Vogler, C. A. Siedlecki, *Biomaterials* **2009**, *30*, 1857.
[8] J. M. Ortega, J. Hartman, J. N. Rodriguez, D. J. Maitland, *Ann. Biomed. Eng.* **2013**, *41*, 725.
[9] V. R. Kumar, S. L. Robbins, *Robbins Basic Pathology*, 8th ed., Saunders/Elsevier, Philadelphia, PA, USA **2007**.
[10] J. N. Rodriguez, M. W. Miller, A. Boyle, J. Horn, C.-K. Yang, T. S. Wilson, J. M. Ortega, W. Small, L. Nash, H. Skoog, D. J. Maitland, *J. Mech. Behav. Biomed. Mater.* **2014**, *40*, 102.
[11] V. M. Donnelly, A. Kornblit, *J. Vac. Sci. Technol., A* **2013**, *31*, 050825.
[12] F. Egitto, F. Emmi, R. Horwath, V. Vukanovic, *J. Vac. Sci. Technol., B* **1985**, *3*, 893.
[13] M. A. Hartney, D. W. Hess, D. S. Soane, *J. Vac. Sci. Technol., B* **1989**, *7*, 1.
[14] C. J. Mogab, A. C. Adams, D. L. Flamm, *J. Appl. Phys.* **1978**, *49*, 3796.
[15] P. K. Chu, J. Y. Chen, L. P. Wang, N. Huang, *Mater. Sci. Eng. R-Rep.* **2002**, *36*, 143.
[16] Y. Ikada, *Biomaterials* **1994**, *15*, 725.
[17] T. Desmet, R. Morent, N. De Geyter, C. Leys, E. Schacht, P. Dubruel, *Biomacromolecules* **2009**, *10*, 2351.
[18] R. Morent, N. De Geyter, M. Trentesaux, L. Gengembre, P. Dubruel, C. Leys, E. Payen, *Plasma Chem. Plasma Process.* **2010**, *30*, 525.
[19] Y. Ozdemir, N. Hasirci, K. Serbetci, *J. Mater. Sci.: Mater. Med.* **2002**, *13*, 1147.
[20] J. J. A. Barry, M. M. C. G. Silva, K. M. Shakesheff, S. M. Howdle, M. R. Alexander, *Adv. Funct. Mater.* **2005**, *15*, 1134.
[21] J. Yang, J. Bei, S. Wang, *Biomaterials* **2002**, *23*, 2607.
[22] S. M. Mukhopadhyay, P. Joshi, S. Datta, J. Macdaniel, *Appl. Surf. Sci.* **2002**, *201*, 219.
[23] C. X. Wang, Y. Liu, H. L. Xu, Y. Ren, Y. P. Qiu, *Appl. Surf. Sci.* **2008**, *254*, 2499.
[24] M. Zelzer, D. Scurr, B. Abdullah, A. J. Urquhart, N. Gadegaard, J. W. Bradley, M. R. Alexander, *J. Phys. Chem. B* **2009**, *113*, 8487.
[25] L. De Nardo, R. Alberti, A. Cigada, L. Yahia, M. C. Tanzi, S. Fare, *Acta Biomater.* **2009**, *5*, 1508.
[26] X. Fu, M. J. Jenkins, G. Sun, I. Bertoti, H. Dong, *Surf. Coat. Technol.* **2012**, *206*, 4799.
[27] P. Abraham, G. Leftheriotis, B. Desvaux, M. Saumet, J. L. Saumet, *Eur. J. Appl. Physiol. Occup. Physiol.* **1994**, *69*, 305.
[28] Y.-J. Yu, K. Hearon, T. S. Wilson, D. J. Maitland, *Smart Mater. Struct.* **2011**, *20*, 085010.
[29] P. Singhal, A. Boyle, M. L. Brooks, S. Infanger, S. Letts, W. Small, D. J. Maitland, T. S. Wilson, *Macromol. Chem. Phys.* **2013**, *214*, 1204.
[30] P. Van der Valk, A. Van Pelt, H. Busscher, H. De Jong, C. R. Wildevuur, J. Arends, *J. Biomed. Mater. Res.* **1983**, *17*, 807.